Chapter 5

Gd-Doped Superparamagnetic Magnetite Nanoparticles for Potential Cancer Theranostics

Maheshika Palihawadana-Arachchige, Vaman M. Naik, Prem P. Vaishnava, Bhanu P. Jena and Ratna Naik

Additional information is available at the end of the chapter

http://dx.doi.org/10.5772/intechopen.68219

Abstract

Nanotechnology has facilitated the applications of a class of nanomaterials called superparamagnetic iron oxide nanoparticles (SPIONs) in cancer theranostics. This is a new discipline in biomedicine that combines therapy and diagnosis in one platform. The multifunctional SPIONs, which are capable of detecting, visualizing, and destroying the neoplastic cells with fewer side effects than the conventional therapies, are reviewed in this chapter for theranostic applications. The chapter summarizes the design parameters such as size, shape, coating, and target ligand functionalization of SPIONs, which enhance their ability to diagnose and treat cancer. The review discusses the methods of synthesizing SPIONs, their structural, morphological, and magnetic properties that are important for theranostics. The applications of SPIONs for drug delivery, magnetic resonance imaging, and magnetic hyperthermia therapy (MHT) are included. The results of our recent MHT study on Gd-doped SPION as a possible theranostic agent are highlighted. We have also discussed the challenges and outlook on the future research for theranostics in clinical settings.

Keywords: theranostics, Fe_3O_4 nanoparticles, MRI contrast agent, drug delivery, magnetic hyperthermia

1. Introduction

Nanomaterials, with the size of at least one dimension ranging from a few nanometers to about a hundred nanometers, having unique properties compared to their respective bulk materials, are of intense research interest because of their applications in various fields of science and technology. One of the major applications, among many of their potential applications, is in biomedicine as platform for effective diagnosis and therapy [1–3]. The multifunctionality of

these nanoparticles has recently led the biomedicine research in a new direction called "Theranostics" which is the integration of diagnostic imaging and therapeutic function into a single platform [4, 5]. Theranostic agents allow the combination of diagnosis, treatment, and follow-up of a disease and hence are expected to contribute to personalized medicine. Among many nanomaterials, magnetic nanoparticles (MNPs) have the potential to deliver imaging and therapeutic agents to a specific region in the body with an external magnetic field manipulation. This requires large magnetization for the MNP so that they could respond to externally applied magnetic fields at physiological temperatures. Superparamagnetic iron oxide nanoparticles (SPIONs), such as Fe_3O_4 and γ-Fe_2O_3 nanoparticles, exhibit relatively higher saturation magnetization with no magnetic hysteresis (zero remanence and coercivity) and fulfill other major requirements such as low toxicity, biocompatibility, and surface functionalization capabilities for theranostic applications. A number of SPIONs have undergone clinical trials and several formulations have been approved for clinical imaging and therapeutic applications [6]. A few examples are Lumiren for bowel imaging, Ferridex IV for liver and spleen imaging, Combidex for lymph node metastases imaging, and Ferumoxytol for iron deficiency therapy.

Furthermore, SPIONs can be multipurposely used for diagnosis such as magnetic resonance imaging (MRI) and for therapeutic functions such as targeted delivery of therapeutic agents, anticancer drugs, siRNA, and for magnetic hyperthermia (MHT) for cancer treatments. This makes SPION an ideal vehicle in the development of theranostic nanomedicine [7–9]. An example of strategy for using magnetic nanoparticles as a potential theranostic agent is illustrated in **Figure 1**.

In this chapter, we discuss the detailed background on magnetic properties of SPIONs and their synthesis methods and surface modification for cancer diagnosis and therapy. In addition, various applications of SPION ranging from MRI contrast agent to therapeutic-targeted drug delivery and MHT are discussed. We have also highlighted the results of our recent study on Gd-doped SPION as a possible theranostic agent. The remainder of the chapter focuses on the challenges and outlook on the future research for theranostics in clinical settings.

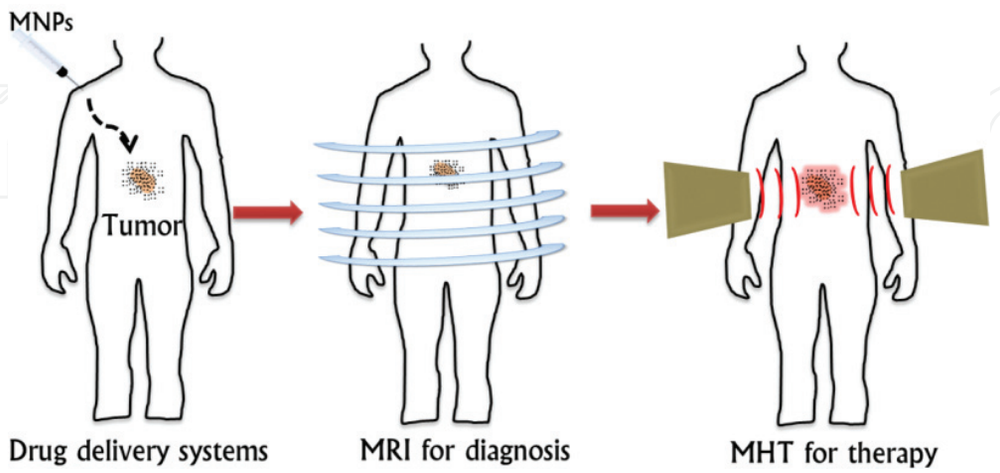

Figure 1. Schematic illustration of the therapeutic strategy using MNP. Functionalized MNPs accumulate in the tumor tissues via the drug delivery system. MNP can be used as a tool for cancer diagnosis by MRI or for magneto-impedance sensor. Hyperthermia can then be induced by alternating magnetic field exposure.

http://dx.doi.org/10.5772/intechopen.68219

2. Magnetic properties of SPION

2.1. Background

MNPs have been studied for over 50 years now due to their potential application in many areas including biomedical sciences. As for the types of MNP, the major focus has been on iron oxide (Fe_3O_4), gold-coated iron oxide (Au-Fe_3O_4), metallic iron (Fe), and Fe-Co and Fe-Pt nanoparticles. In most cases, the particle size ranges from 1 to 100 nm exhibiting high surface-to-volume ratio. As a result, they offer higher surface area for interaction with foreign objects compared to larger particles. Many review articles have been written that focus on sensing, drug delivery, and hyperthermia properties of these nanoparticles [10–13]. The physical, chemical, and magnetic properties of MNP largely depend on synthesis method and their surface modification, and much progress has been made in this direction to MNP of varying sizes, shapes, composition, and core-shell designs [14–23].

The important magnetic parameters relevant to theranostic applications are saturation magnetization (M_s), remanent magnetization (M_r), coercivity (H_c), Curie temperature (T_c), magnetic anisotropy energy density (K), and blocking temperature (T_b). These parameters are influenced by the material, size, shape, composition, and core-shell (functionalization) of the nanoparticles. M_s is the maximum value of magnetization of the material that can be achieved under the influence of an external magnetic field, M_r is the remanent magnetization in the material after removing the external magnetic field, H_c is the strength of the reverse magnetic field needed to bring the remanent magnetization to zero, and K is the material property signifying the tendency of the magnetization to orient along a certain axis of the particle. As the volume (V) of the particles decreases, the magnetic anisotropy energy (KV) of the nanoparticle also decreases. If the particle size is reduced below a certain critical size, it becomes a single magnetic domain creating a giant spin called "superspin" leading to a large magnetic moment (~10,000 Bohr magneton) on each particle. The behavior of a collection of such noninteracting particles under an external magnetic field is determined by a competition between the magnetic anisotropy energy barrier (ΔE) and the thermal energy (k_BT) for magnetic moment reversal. Above a characteristic temperature called the blocking temperature, T_B, their behavior is very similar to that of a paramagnetic material and described as "superparamagnetism." The underlying physics of superparamagnetism is founded on the activation law for the relaxation time τ of the net magnetization of the particle given by $\tau = \tau_o \exp(\Delta E/k_BT)$, where τ_o is of the order of 10^{-9}–10^{-12} s [24].

2.2. Effect of size, shape, and composition

Magnetic properties of materials, such as susceptibility, coercivity, and saturation magnetization, depend on the structure, size, shape, and composition, and can be altered to manipulate the magnetic properties. Particle size plays an important role in many magnetic biomaterial applications such as magnetic hyperthermia and drug delivery, where the size used lies in the nanometer regime. The MNPs often contain a layer of disordered spins on the surface of the particle leading to reduction in their M_s compared to the corresponding bulk material. A relation between the M_s and the size of the nanoparticle is given by [25]

$$M_s = M_{sb}\left(\frac{r-d}{r}\right)^3 \quad (1)$$

where r is the radius of the nanoparticle, d is the layer thickness of the disordered spins, and M_{sb} is the saturation of the bulk material. Recent studies have shown that the functionalization of MNP can reduce the thickness of the surface-disordered spin layer [26].

Although the effect of shape of MNP on their magnetic properties is not extensively studied, a few investigations have been reported in the literature on ferrite nanocubes, maghemite nanorods, NiFe wires, cobalt nanodiscs, tetrapods, and Au-MnO nanoflowers showing a strong dependence of M_s on the shapes of the nanoparticles [27–36]. Higher M_s values have been observed for the cubic MNP compared to the spherical MNP of the same size [37]. Also, cubic Fe_3O_4 nanoparticles have been found to exhibit higher T_B compared to spherical Fe_3O_4 nanoparticles [38], and the amount of disordered spins to be less (4%) in the former and more (8%) in the latter [39].

Magnetic properties of widely used magnetite (Fe_3O_4) with its spinel structure of $[Fe^{3+}]_A[Fe^{3+}Fe^{2+}]_BO_4$ can be changed if other magnetic atoms such as Ni, Co, Mn, and so on are substituted at the tetrahedral A or octahedral B sites of the spinel structure. This flexibility of creating mixed ferrites is useful in tuning the magnetic properties for hyperthermia applications. There have been numerous studies investigating the interdependence of magnetic properties and the composition. The method of preparation, concentration and nature of dopants, and postsynthesis processes have shown to profoundly affect the magnetic properties. A study [40] compared the magnetization among the four spinels of $FeFe_2O_4$, $MnFe_2O_4$, $CoFe_2O_4$, and $NiFe_2O_4$ for the same size of 12 nm and found the highest magnetization for $MnFe_2O_4$. In another study with $Y_3Fe_{5-x}Al_xO_{12}$ for x varying between 0 and 2, the Curie temperature changed from 40 to 280°C [41]. With increasing Al, Fe^{3+} cations occupied the tetrahedral sites and some of the octahedral sites of Fe^{2+} were replaced by nonmagnetic Al^{3+} cations, which reduced the magnitude of M_s. The T_c value reached the room temperature for x value between 1.5 and 1.8. The variation in composition affects not only the magnitude of M_s but also the coercivity. The tailoring of ferromagnetic to paramagnetic phase transition temperature is particularly very useful in hyperthermia application to turn off undesirable heating beyond the required temperature.

3. SPION synthesis and surface modification

Over the past decades, many efficient synthesis methods have been developed to produce the size/shape controlled, stable, biocompatible, and monodispersed iron oxide nanoparticles [42–45]. The most common methods include coprecipitation [46, 47], thermal decomposition [48], hydrothermal synthesis [49, 50], microemulsion [51], and sonochemical [52] synthesis. Thermal decomposition technique involves decomposition of organo-metallic iron precursors in organic solvents at higher temperatures. Although the method can produce high-quality monodisperse particles because of separate nucleation and growth processes, it is a complicated synthesis method and

produces hydrophobic nanoparticles that cannot be directly used for bio-applications without laborious postsynthesis processes, which may result in aggregation and loss of magnetic properties. The most commonly used technique is the coprecipitation method, which is a cost-effective and a facile synthesis method. However, this method produces Fe_3O_4 nanoparticles with wide particle size distribution due to lack of control over hydrolysis reactions of the iron precursors, and the nucleation and growth steps leading to particles with a range of superparamagnetic-blocking temperature. The other common, recently developed, method is the hydrothermal synthesis, which generates nanoparticles with excellent crystallinity with controllable size and shape in aqueous phase. The properties of the nanoparticles can vary with the synthesis method due to the differences in cationic distribution and vacancies, spin canting, or surface contribution.

In the design of magnetic nanoparticles for theranostic applications, surface modification plays an important role in providing colloidal stability and biocompatibility. The stable colloidal suspensions of surfactant-coated SPION are called "ferrofluids" which are magnetizable and remain as liquids in the presence of magnetic fields and in biological media. Stabilization of the ferrofluid occurs in the presence of one or both of the two repulsive forces (see **Figure 2**). The electrostatic repulsion can be understood through the knowledge of the diffusion potential and mainly depends on the ionic strength and the pH of the solution. The steric force is difficult to predict or quantify and mostly depends on the weight and the density of the polymer used for the coating.

In order to achieve biocompatibility, the coating should prevent any toxic ion leakage from magnetic core into the biological environment as well as shielding the magnetic core from oxidation and corrosion. When nanoparticles are injected into the body during in vivo applications, they are often recognized by reticuloendothelial system (RES) that eliminates any foreign substance from blood stream [53]. In this process, nanoparticles are rapidly attacked by the plasma proteins from RES and shuttled out of circulation to the liver, spleen, or kidney,

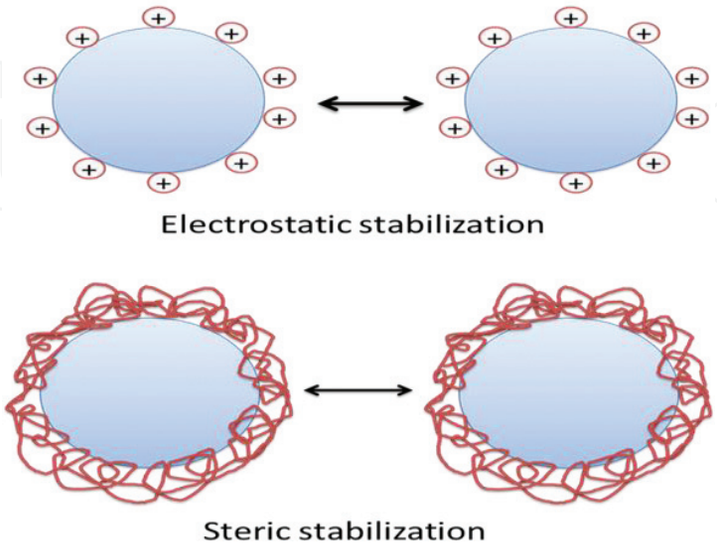

Figure 2. Electrostatic and steric repulsion between the particles.

which are then cleared out from the body. Also, this RES accumulation often causes toxicity issues as well. The specific surface coatings can prevent the adsorption of these proteins, increasing the circulation time in blood, hence maximizing the possibility to reach target tissues [54]. For instance, it is well known that coating of hydrophilic polymers, mainly polyethylene glycol (PEG), on the nanoparticles reduces nonspecific binding of the proteins resulting in stealth behavior. In addition to the stabilization and enhanced biocompatibility, these protecting shells also provide a platform for further functionalization such as the addition of specific targeting ligands, dyes, or therapeutic agents.

Over the years, researchers have developed various surface modification strategies composed of grafting of or coating with both organic and inorganic materials. Organic molecules include small organic molecules, macromolecules or polymer and biological molecules. They provide various highly reactive functional groups such as carboxyl groups, aldehyde groups, and amino groups. Polymer-coating materials can be classified into synthetic and natural, and some commonly used polymers are listed in **Table 1** along with their advantages.

The surface coating could affect the magnetic properties of SPION. Many studies have reported the effect of the surfactants on the magnetic properties [55–60]. Yuan et al. [58] investigated the effect of surfactant on magnetic properties using commercially available aqueous nanoparticle suspensions, FluidMAG-Amine, FluidMAG-UC/A, and FluidMAG-CMX, in parallel with oleic acid-covered particles suspended in hexane and heptane. Their results reveal the reduction of magnetic phase in nanoparticles, which varies with different coatings as well as with solvents. The reduction in magnetization with different coatings was attributed to the different degree of surface spin disorder.

Polymer		Advantages and applications	References
Natural	Dextran	Stability, biocompatibility, enables optimum polar interactions with iron oxide surfaces, and enhances the blood circulation time	[61–66]
	Starch	Improves the biocompatibility, good for MRI, and drug target delivery	[67, 68]
	Chitosan	Biocompatible and hydrophilic large abundance in nature, biocompatibility, and ease of functionalization. widely used as nonviral gene delivery system	[69–72]
Synthetic	Poly(ethylene-glycol) (PEG)	Enhances the hydrophilicity and water-solubility, improves the biocompatibility, blood circulation times, and internalization efficiency of the nanoparticles. Used in target-specific cell labeling, magnetic hyperthermia, targeted drug delivery	[73–75]
	Alginate	Improves the stability and biocompatibility. Used in drug delivery applications	[76–78]
	Poly-N-isopropyl-acrylamide (PNIPAM)	Generally used as thermosensitive drug delivery and cell separation	[79–82]
	Polyethylene-imine (PEI)	Ability to complex with DNA, guide intracellular trafficking of their cargo into the nucleus, used for gene delivery cell transfection with either DNA or siRNA nucleotides	[83–86]

Table 1. Commonly studied organic polymers and their advantages.

4. SPION for drug delivery

Over the last two decades, MNPs have been increasingly exploited as platforms for the transport of therapeutics including drugs and genes [46, 87, 88]. In magnetic drug delivery, a drug or a therapeutic reagent is conjugated to the nanoparticle and introduced in the body, and concentrated in the target area by means of a magnetic field gradient (using an internally implanted permanent magnet or an externally applied field) [89]. Even though magnetic drug delivery shows a great promise in cancer treatment avoiding the side effects of conventional chemotherapy, the designing and fabrication of an efficient nanoparticle-based drug delivery system is still a challenge. Using a targeting ligand, the targeting specificity can be enhanced. These anticancer drugs carried by the nanoparticles can then be released at the tumor site via enzymatic activity, or via changes in the physiological conditions such as temperature and pH. Drug release can also be magnetically triggered from the drug-conjugated magnetic nanoparticles [89–91]. For example, Hayashi et al. [92] reports a study done on superparamagnetic iron oxide nanoparticles conjugated with folic acid (well known as a targeting ligand for breast cancer cells), β-Cyclodextrin (which acts as drug container), and Tamoxifen (anticancer drug). Using an AC magnetic field, heat is generated which triggers drug release—a behavior that is controlled by switching the high-frequency magnetic field on and off. This is capable of performing drug delivery and hyperthermia simultaneously. Among various other anticancer drugs, Doxorubicin (Dox) is widely used as a model drug. There are several methods that can be used to load Dox into nanoparticles, such as by adsorption onto nanocarrier inorganic core [93–95], by diffusion [95, 96], or entrapment [97, 98] in the coating materials and by chemical bonds [99, 100] with the coating of the nanocarrier. Several modifications including surface functionalization of these SPIONs with Dox have been conducted over the last few years to investigate their efficacy [101]. Previous studies have reported that PEG-functionalized porous silica shell onto Dox-conjugated Fe_3O_4 nanoparticle cores [102], PAMAM (Poly(amidoamine))-coated Fe_3O_4 nanoparticles-Dox complex [103], and Dox-loaded Fe_3O_4 nanoparticles modified with PLGA-PEG copolymers [104] could potentially be very promising in therapeutic cancer treatment. However, most of the Dox-SPION–based drug delivery studies have been focused on human breast cancer cells.

In our recently published work [105], we have developed a novel drug delivery platform based on Fe_3O_4 nanoparticles as a vehicle for an anticancer drug (Dox), attached to a model dye (FITC) for their precise tracking and investigated their incorporation into the human pancreatic cancer cell line (MIA PaCa-2) for specific drug targeting. Existing EDC/NHS technique was employed for this dual drug/dye conjugation. This unique drug-dye dual conjugation of SPION after penetration through the cell membrane shows a steady release of Dox into the nucleus of the malignant cells. Our studies demonstrate that the association of Dox onto the surface of nanoparticles enhances its penetration into the cancer cells as compared to the unconjugated drug as shown in the subsequent text (**Figure 3**). In addition to the rapid uptake of these SPIONs by live cells, our results also suggest that upon entering the cells, Dox is cleaved from the conjugation, which might be due to the enzymatic reactions that occur within the cells, and tends to accumulate in the nuclei fulfilling the major requirement for an effective therapeutic system.

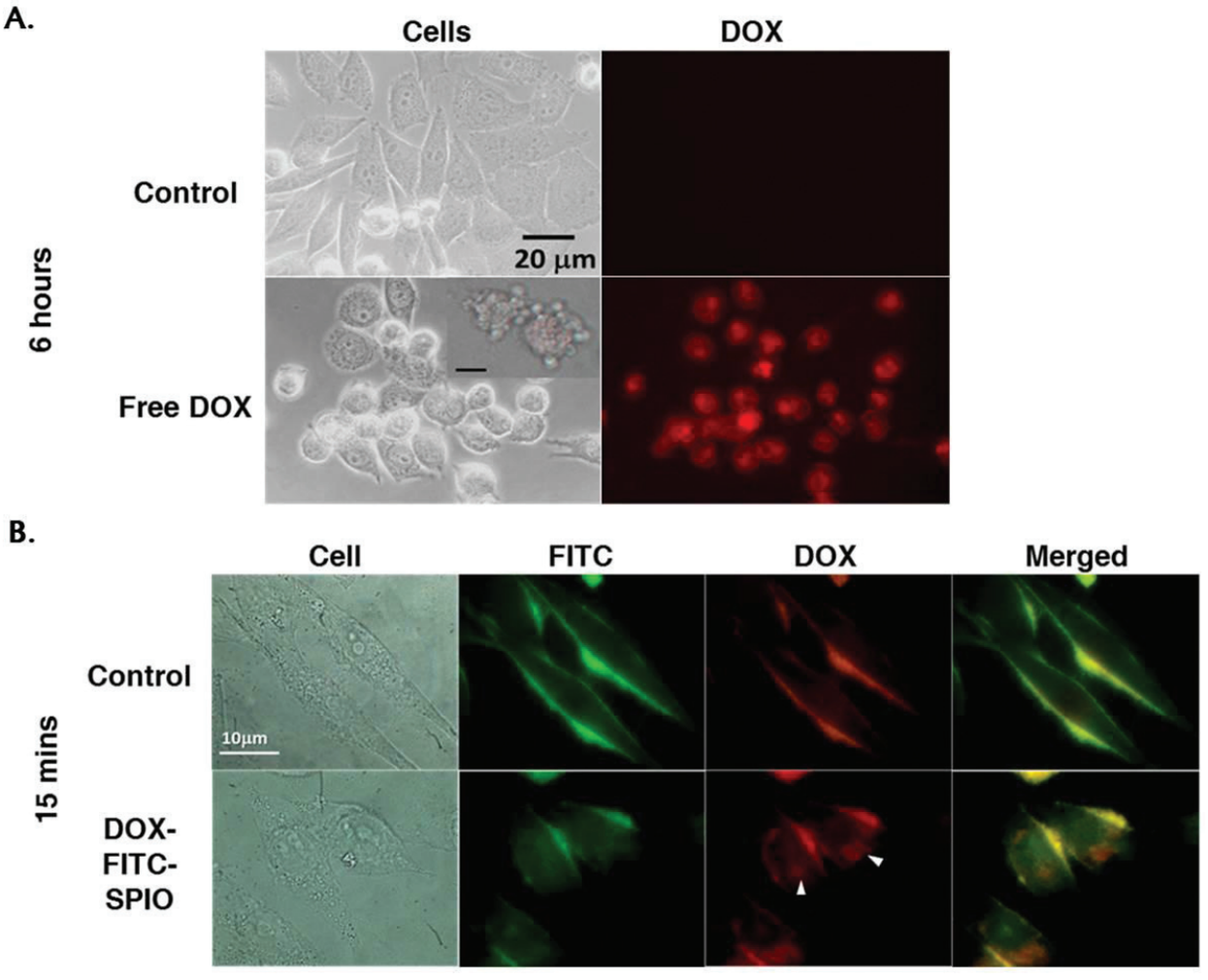

Figure 3. (A) Phase and fluorescent micrograph of MIA PaCa 2 cells incubated with Dox. Note the cellular entry, especially into the nucleus (red fluorescence), of the free drug 6 h following exposure. The inset shows blebbing of cells exposed to Dox prior to cell death (Scale = 20 μm). (B) Phase and fluorescent micrograph of MIA PaCa 2 cells incubated with free Dox and free FITC (control) and Dox-FITC-conjugated Fe_3O_4 NPs at 15 min. Green and red fluorescence represent FITC and Dox, respectively. Note the accumulation of Dox in the nucleus in cells exposed to the Dox and FITC-conjugated SPION. White arrowheads indicate Dox entry into the nucleus. Reprinted from Ref. [105], Copyright (2017), with permission from Elsevier.

5. SPION for cancer diagnosis using MRI

Magnetic resonance imaging with its high spatial resolution has been a preferred method of imaging and diagnosing a disease. It is a noninvasive medical diagnostic tool that monitors the change in magnetization of hydrogen-protons in water molecules contained in a tissue when placed in a magnetic field and exposed to a pulse of radio frequency electromagnetic waves. The mapping of the magnetization provides an image of the organ due to the fact that protons in different tissues, with varying water concentration, respond differently. Contrast agents have been used to enhance the images as they affect the behavior of the protons in their vicinity leading to sharper images. Contrast agents used in MRI are divided into two categories: T_1 and

T_2 contrast agents based on their effect on the magnetic relaxation processes of the protons [106]. Most commonly used T_1 contrast agents are paramagnetic compounds that are composed of metal ions of Gd^{3+} or Mn^{2+} and a chelating ligand, such as diethylene triamine penta-acetic acid, DTPA [106, 107]. The chelate prevents the metal ion from binding to chelates in the body making the paramagnetic ion less toxic. T_1 contrast agents mainly reduce the longitudinal relaxation time (T_1) which is due to energy exchange between the spins and surrounding lattice (spin-lattice relaxation) and result in a brighter signal. T_2 contract agents, consisting of superparamagnetic nanoparticles such as Fe_3O_4, have a strong effect on the transverse relaxation time (T_2). In an external magnetic field, nanoparticles are magnetized and generate induced magnetic fields locally. These induced fields perturb the magnetic relaxation processes of the protons in the water molecules decreasing the T_2 relaxation time, which results in darkening of MR images.

There are various research studies conducted on enhancing the MRI signal for cancer detection using SPIONs as T_2 contrast agents [108–110]. The efficiency of SPIONs as T_2 contrast agents mainly depends on their physicochemical properties, particularly their size and surface chemistry. Stephen et al. [111] report the correlation between particle size and T_2 relaxation. Their study shows that a decrease in particle size leads to reduction in saturation magnetization, which in turn reduces the T_2 relaxation capabilities of SPIONs. There are studies which show the effect of shape on relaxivity. For example, Zhen et al. [112] reported that cubic Fe_3O_4 MNP showed four times smaller relaxation time and thus better image contrast compared to the spherical Fe_3O_4. In another study, octapod Fe_3O_4 nanoparticles with an edge length of 30 nm show a smaller value of T_2 compared to 16-nm spherical Fe_3O_4 nanoparticles possessing a similar M_s [37]. The studies by Park et al. [113] report a decrease in relaxivity as PEG molecular weight increases, indicating that the thickness of PEG coating at the particle surface affects T_2 relaxivity.

When using SPIONs as contrast agents for MRI, it is crucial that they are captured into the cells efficiently upon exposure. Some approaches include introducing peptides [114], antibodies [115], and polymers [116] onto or surrounding magnetic nanoparticles to improve the target specificity. For example, Jun et al. [117] have successfully synthesized superparamagnetic iron oxide nanoparticles of 9-nm size as magnetic probes for the in vivo detection of cancer cells implanted in a mouse. In their research work, 2,3-dimercaptosuccinic acid (DMSA) ligand is attached to the nanoparticles surface to obtain hydrophilic nanoparticles and the nanoparticles are further conjugated with the cancer-targeting antibody, Herceptin. The specific binding properties of Herceptin against a HER2/neu receptor overexpressed from breast cancer cells lead to the successful detection of breast cancer cells (SK-BR-3).

Even though both T_1 and T_2 mapping are powerful techniques, single-mode contrast agents are not always sufficient in modern diagnosis as they have certain drawbacks and limitations [118]. For example, the dark contrast produced by T_2 agents can also be generated from adjacent bones or vascular or there can be susceptibility artifacts due to the sharp change in magnetic field at the surrounding contrast agent. Also, Gd-chelates (T_1 agent) have high mobility which shorten their presence in the vascular system and raise possible toxicity issues. Thus, there is a growing interest in developing complementary T_1-T_2 dual-modal contrast agents, combining the advantages of

positive and negative contrasts to obtain high sensitivity and biocompatibility for improved diagnosis [119]. Two different approaches of integrating T_1 and T_2 species have been reported recently [118]. One is constructed by labeling T_1-signaling elements (Gd species) on magnetic nanoparticles. In the study done by Bae et al. [120], Gd-DTPA, a representative Gd chelate-based T_1 MRI contrast agent, is covalently attached to dopamine-coated iron oxide nanoparticles. Their results demonstrated that the composite not only had the ability to improve surrounding water proton signals on the T_1-weighted image but also could induce significant signal reduction on the T_2-weighted image. In another study reported by Santra et al. [121], Gd-DTPA is encapsulated within the poly (acrylic acid) (PAA) polymer-coated SPION (IO-PAA) conjugated to folic acid, which acts as the targeting ligand for breast cancer cells (HeLa cells). When nanoprobes are internalized within the cells, which is acidic, composite magnetic nanoprobe degrades resulting in an intracellular release of Gd-DTPA complex with subsequent T_1 activation, which can be seen by MRI. Authors claim that this T_1 nano-agent could be used for the detection of acidic tumors. The other type of conjugated system consists of T_1 paramagnetic elements embedded into T_2 magnetic nanoparticles. For example, Zhou et al. [122] have synthesized Gd_2O_3-embedded iron oxide nanoparticles with an overall size of 14 nm which can act as a T_1-T_2 mutually enhanced dual-modal contrast agent for MR imaging of liver and hepatic tumor detection with great accuracy in mice. Xiao et al. [123] have prepared PEGylated, Gd-doped iron oxide nanoparticles which is applicable as a T_1-T_2 dual-modal MRI contrast agent. Their in vivo MRI results demonstrated the simultaneous contrast enhancements in T_1- and T_2-weighted MR images toward the glioma-bearing mice.

6. SPION for cancer therapy using magnetic hyperthermia

Magnetic hyperthermia is the transformation of electromagnetic energy from an external alternating magnetic field into heat using MNP. Magnetic nanoparticles serve as the nano-heat centers producing heat by relaxation losses, thereby heating the tissue. The main goal of an effective cancer treatment is to kill the malignant cells with the least of damage to normal cells. As MHT can be used for heating small regions selectively, it offers the potential for being highly selective and noninvasive technique for therapeutic treatment of cancers, and consequently it has advantage over other treatment such as chemotherapy and radiation therapy. It is known that reduced blood flow in tumor causes the lack of oxygen in tumor site which leads to the formation of lactic acid making the cells more acidic [124]. The acidic cells are more sensitive to temperature, have lower thermal resistance than normal cells, and the decreased blood flow in the tumor limit their ability to dissipate heat. As a result, cancer cells can be damaged or killed by increasing the local temperature to the range of 42–46°C with little detriment to healthy cells.

The idea of utilizing SPION for hyperthermia was first proposed by Gilchrist et al. [125] in 1950s and since then many types of MNP are being investigated for this purpose. MNPs have the advantage of being guided and localized specifically at a tumor site by external magnetic fields and can also be directed to the cancer cells by tagging a ligand, such as an antibody or a peptide, without reducing its efficiency. For example, Fabio et al. [126] have reported that the conjugation of folate receptors enhances the targeting for magnetic hyperthermia in solid

tumors. Magnetite (Fe_3O_4) and maghemite (γ-Fe_2O_3) have been extensively studied and are promising candidates due to their biocompatibility and relative ease for functionalization. Additionally, iron oxide nanoparticles doped with other magnetic dopants such as Co, Mn, and Ni [127–129] are under investigation to achieve a high heating efficiency by tuning the magnetic anisotropy and saturation magnetization of the material. In addition, many recent findings show that multicore nanoparticles possess a higher heating power than the single-core particles [130], and may offer an advantage. However, among numerous complications, with a high Curie temperature of Fe_3O_4, 850 K, and γ-Fe_2O_3, 750 K, overheating is one of the drawbacks of utilizing these nanoparticles, and as a solution, those complex magnetic oxides with low Curie temperature are being investigated [131–133].

Specific absorption rate (SAR) is a measure of efficiency of heat generation. The SAR value can be estimated by measuring the temperature change in the ferrofluid samples upon exposure to an AC magnetic field following the equation [134]:

$$SAR(T) = \frac{M_{sample}}{m_{Fe_3O_4}} C \left(\frac{\Delta T}{\Delta t}\right)_T \tag{2}$$

Here, M_{sample} is the mass of the sample, $m_{Fe_3O_4}$ is the mass of Fe_3O_4 nanoparticles in the sample, C is the specific heat capacity of the sample, and $\left(\frac{dT}{dt}\right)_T$ is the time rate of change of temperature at T obtained from the slope of the time-dependent temperature data. SAR depends on magnetic properties of the particles such as M_s, anisotropy constant K, particle size distribution (σ), magnetic dipolar interactions, and the rheological properties of the target medium. An ensemble of poly-disperse particles is usually described by a log-normal distribution function,

$$f(D) = \frac{1}{\sqrt{2\pi}\sigma D} \exp\left\{-\frac{[\ln(D/D_\circ)]^2}{2\sigma^2}\right\} \tag{3}$$

Here, D_o is the most probable particle diameter and σ is the width of the distribution. The temperature-dependent average power dissipation in the sample is expressed as [135]

$$\overline{P}(T) = \int_0^\infty \frac{\mu_0 \chi_0 H_0^2 \omega}{2} \frac{\omega \tau_{eff}}{1 + (\omega \tau_{eff})^2} f(D) d(D) \tag{4}$$

where H_o and ω are the amplitude and angular frequency of the applied AC magnetic field, μ_o is the vacuum permeability, τ_{eff} is the effective relaxation time involving Néel relaxation and the Brownian relaxation times, and χ_o is equilibrium susceptibility. τ_{eff} is defined as $\frac{1}{\tau_{eff}} = \frac{1}{\tau_N} + \frac{1}{\tau_B}$, where $\tau_B = \frac{4\pi\eta R_H^3}{k_B T}$ and $\tau_N = \frac{\sqrt{\pi}}{2}\tau_0 \exp\left(\frac{KV}{k_B T}\right)\sqrt{\frac{KV}{k_B T}}$ are the Néel and Brownian relaxation times, η is the viscosity of the suspension, R_H is the hydrodynamic radius of the coated nanoparticle, V_m is the magnetic volume of the nanoparticles, and $\tau_o \sim 10^{-9}$ s. χ_o is given by $\chi_o = \chi_i\left(\coth\xi - \frac{1}{\xi}\right)$, where $\chi_i = \frac{\mu_\circ \phi M_d^2 H_\circ V_m}{3k_b T}$ is the initial susceptibility, and $\xi = \frac{\mu_\circ M_d H_\circ V_m}{k_b T}$, with M_d being the domain magnetization of the nanoparticle and ϕ the volume fraction of the magnetic nanoparticles in the ferrofluid. SAR in units of W/g is obtained using Eq. (4) as $\overline{P}(T)/m_{Fe_3O_4}$, where $m_{Fe_3O_4}$ is the mass of Fe_3O_4 nanoparticles in ferrofluids.

MHT investigations are often done on colloidal suspensions of surface-coated MNP, called ferrofluids. It is often necessary to coat the MNP using a biocompatible polymer to avoid direct contact with the tissue and to reduce the particle aggregation. Ferrofluid preparations frequently yield a mixture of isolated nanoparticles and nanoclusters [136] with varying degree of magnetic dipole-dipole interactions present in ferrofluids. It has been shown that the dipolar interactions among the MNP affect the SAR value drastically and can be exploited to optimize SAR [136–139]. A mean-field approximation method has been used to account for effects of interactions on SAR for a collection of monodisperse MNP [138, 139], and we have used this approach to explain the very different observed SAR values for similar size particles prepared by two different methods of preparation [140].

Since the surfactant influences the magnetic properties as well as the degree of interactions in the ferrofluid, a useful approach for improving the magnetic hyperthermia performance is to optimize the surface coating to maximize the SAR. Currently, there are conflicting SAR values obtained for a certain sized nanoparticle making it difficult to evaluate the exact contributions of surface coating on the SAR. According to Mohammad et al. [141], it is found that inorganic coatings improve the SAR value and the gold coating retains the superparamagnetic fraction of Fe_3O_4 nanoparticles much better than uncoated nanoparticles alone and leads to higher magnetocrystalline anisotropy. A study by Liu et al. [142] suggested the possibility of increasing SAR by decreasing the surface-coating thickness using highly monodispersed Fe_3O_4 nanoparticles with different polyethylene glycol-coating thickness. The increase in SAR was explained as due to a decrease in coating thickness leading to an increased Brownian loss, improved thermal conductivity, as well as improved dispersion. It should be noted that the heating performance of the nanoparticles depends on the medium as well. Whenever nanoparticles encounter biological systems, interactions take place between their surfaces and biological components such as proteins, membranes, phospholipids, and DNA forming the so-called protein corona around the nanoparticles [143, 144]. The formation of corona depends on the surface properties of the particles [145, 146] and can influence the aggregation behavior of nanoparticles in biological media, which in turn can affect their performance for desired applications. Therefore, apart from the optimization of the properties of the magnetic core and surface coating for high-performance MHT, it is necessary to ensure its performance in the physiological environments.

In the work reported by Khandhar et al. [147], authors use poly(maleic anhydride-alt-1-octadecene)-poly(ethylene glycol) (PMAO-PEG), an amphiphilic polymer-coated Fe_3O_4 nanoparticles of three different sizes, 13, 14, and 16 nm, to study the MHT efficiency in cell growth medium (CGM) similar to biological environment. Their results showed an increase in hydrodynamic sizes in all three samples upon exposure to CGM. SAR reduced (30%) only in 16-nm size sample, while other two samples did not exhibit any significant decrease in SAR. The authors suggest that the increase in hydrodynamic volume prolongs Brownian relaxation while Néel relaxation is unaffected. Hence, in 13- and 14-nm samples where SAR is mainly due to Néel relaxation, SAR was not affected. But in the 16-nm samples, in which there is a contribution from Brownian relaxation to heat dissipation, the SAR dropped due to the increase in Brownian relaxation. We have investigated the magnetic hyperthermia efficiency of dextran and citric acid (CA)-coated Fe_3O_4 ferrofluids in cell growth medium, which contains

http://dx.doi.org/10.5772/intechopen.68219

serum proteins similar to physiological environments. From the stock solutions (25 mg/ml), 3 mg/ml concentration of dextran and citric acid-coated ferrofluids samples were prepared using CGM and deionized water (DI) water. The ferrofluid samples were subjected to an AC field of 235-Oe amplitude at the frequency of 375 kHz. The SAR of dextran-coated samples in DI and CGM was estimated to be 63 and 72 W/g, which indicates that their performance is not much affected by the medium if not enhanced. However, SAR values obtained for CA-coated samples in DI and CGM, 78 and 38 W/g, implies that their efficiency is heavily reduced when exposed to physiological environments.

7. Gd-doped SPION as a potential theranostic agent

The multifunctionality of SPION makes them a good candidate for theranostics. One such approach to integrate diagnostic imaging and therapeutic function is to develop SPION as an MRI/a drug delivery platform. Yu et al. [148] reported that PEG-coated iron oxide nanoparticles when loaded with Dox provide a therapeutic capability. Following their injection into a mouse, Dox-modified magnetic nanoparticles accumulate in the tumor and the nanoparticles were imaged by using T_2 MRI. The contrast associated with the tumor changes from light to dark at 4.5 h post injection and the growth rate of the tumor mass was decreased in the nanoparticle-injected mice compared to that of a control group. In another work, Lee et al. [149] developed PEG-stabilized Fe_3O_4 nanocrystals on dye-doped mesoporous silica nanoparticles and Dox was loaded into the pores. Here, SPIONs work as a contrast agent in MRI, the dye molecule imparts optical imaging modality, and Dox induces cell death. In a similar approach, Kim et al. [150] developed a core-shell structure consisting of single Fe_3O_4 core and mesoporous silica shell for MR and fluorescence imaging which also has the potential to be used as a drug carrier. Hayashi et al. [92] reports a study done on SPION conjugated with folic acid as targeting ligand and Tamoxifen as anticancer drug. The drug release was triggered by heat generated by SPION in an AC magnetic field, hence performing drug delivery and hyperthermia simultaneously.

The incorporation of MHT and imaging modalities [151] has been investigated widely as well. One such study is reported by Hayashi et al. [152] in which authors have investigated SPION for cancer theranostics by combining MRI and magnetic hyperthermia through a set of *in vivo* experiments. They show that FA- and PEG-modified SPION nanoclusters accumulated locally in cancer tissues within the tumor and enhanced the MRI contrast. Furthermore, they report that with MHT, the tumor volume of treated mice was reduced to one-tenth that of the control mice. Also, Gd-doped Fe_3O_4 nanoparticles have the potential to act as an effective MHT agent [153] in addition to their use as a T_1-T_2 dual-modal contrast agent for MR imaging. Gd(III) is known to oppose net magnetic moment of Fe(III)/Fe(II) in oxides, reducing magnetization [154–156]. Therefore, Gd doping may reduce the hyperthermia efficiency, but by using the correct amount of doping, one can always explore the possibility of using them as both MRI contrast agents and hyperthermia mediators. However, there are very few studies done on the MHT efficiency of Gd-doped Fe_3O_4 nanoparticles [157, 158]. Both the studies report higher SAR values for Gd-doped Fe_3O_4 nanoparticles compared to the reported values for undoped samples. In our work presented

here, we have investigated the MHT efficiency of $Gd_{0.075}Fe_{2.925}O_4$ nanoparticles for possible use as a theranostic agent.

7.1. Synthesis and characterization of Gd-doped SPION

$Gd_{0.075}Fe_{2.925}O_4$ nanoparticles were synthesized by coprecipitation method. For a typical synthesis of $Gd_{0.075}Fe_{2.925}O_4$, aqueous solution of $FeCl_2.4H_2O$, $FeCl_3.6H_2O$ and $Gd(NO_3)_3$ was mixed in a molar ratio of 1.00:1.925:0.075 in 25-ml volume followed by the addition of 250 ml of 1 M NH_4OH. The synthesized nanoparticles were then coated with dextran according to the method outlined by Arachchige et al. [140]. From the structural investigation, it was observed that Gd doping does not alter the Fe_3O_4 crystal structure significantly (**Figure 4**). Using several intense X-ray diffraction (XRD) peaks and the Debye-Scherer equation, the crystallite sizes of the Fe_3O_4 and $Gd_{0.075}Fe_{2.925}O_4$ nanoparticle samples were determined to be 11.7 ± 0.6 and 14.9 ± 0.5 nm, respectively. This increase in the crystallite size is consistent with the previous studies on Gd doping in spinel structures [159].

TEM images of the two samples are shown in **Figure 5**. The undoped sample consists of roughly spherical nanoparticles with smaller polydispersity, whereas the Gd-doped sample exhibits nanoparticles with rough edges with wider size distribution.

The magnetic properties of the synthesized powder as well as the ferrofluid samples are determined by analyzing the *M*(*H*) curve. The M-H data for undoped and Gd-doped Fe_3O_4 ferrofluid samples, recorded at room temperature, are shown in **Figure 6**. The sigmoidal shape of the *M*(*H*) curves with nearly zero hysteresis confirms the superparamagnetic nature of these nanoparticles at room temperature. The saturation magnetization of Fe_3O_4 nanoparticles is measured to be ~72 emu/g, whereas that of Gd-doped Fe_3O_4 nanoparticles is reduced to ~52 emu/g. This reduction in saturation magnetization at room temperature agrees with the observations in other reported studies [123, 158] and can be attributed to the fact that magnetic Fe^{3+} ions get replaced by the Gd^{3+} ions in the octahedral sites of the inverse spinel structure.

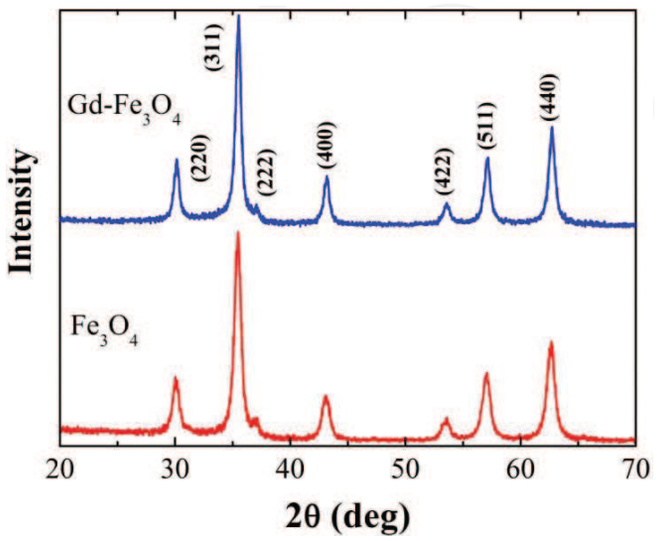

Figure 4. X-ray diffraction patterns of as-prepared Fe_3O_4 and $Gd_{0.075}Fe_{2.925}O_4$ nanoparticles [160].

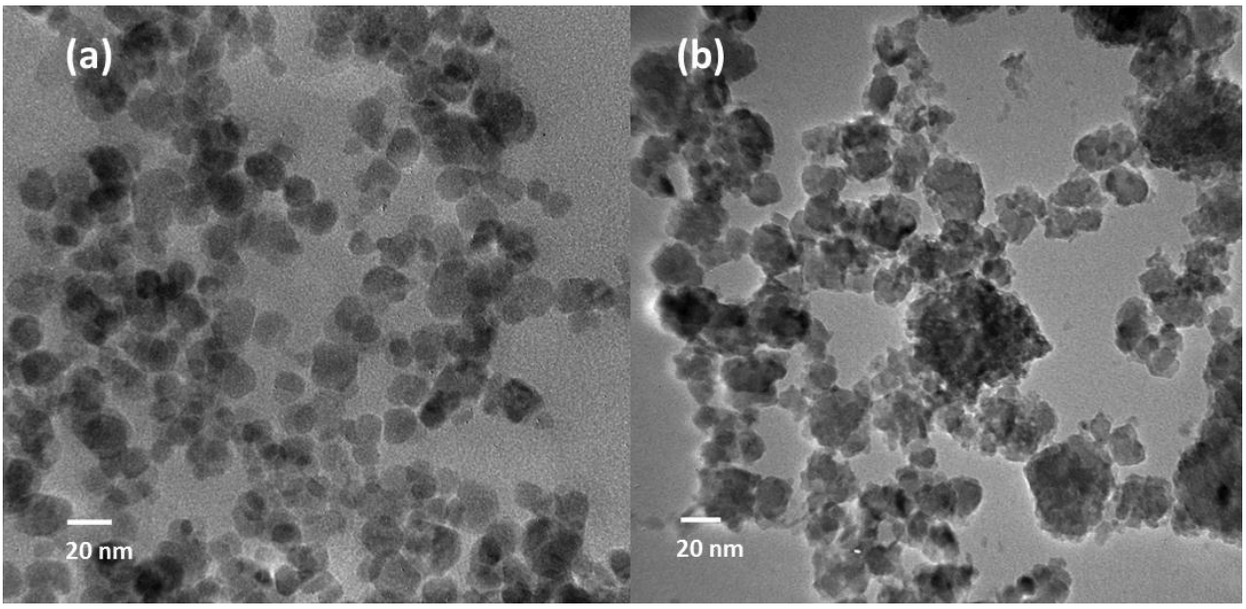

Figure 5. TEM images of (a) Fe_3O_4 and (b) Gd-Fe_3O_4 nanoparticles [160].

It is observed that the doping of Gd^{3+} ions into Fe_3O_4 spinel has significantly influenced the average crystallite size and the saturation magnetization. The $M(H)$ curve for an ensemble of noninteracting superparamagnetic nanoparticles described by a log-normal distribution function, $f(D)$, can be fitted using the following expression:

$$M(H) = M_s \frac{\int_0^\infty f(D)VL(x)dD}{\int_0^\infty f(D)VdD} \tag{5}$$

where $L(x) = \coth x - \frac{1}{x}$ is the Langevin function, $x = (M_s VH)/k_B T$, M_s is the saturation magnetization, and V is the volume of the particle. The fitted particle size was inconsistent with the

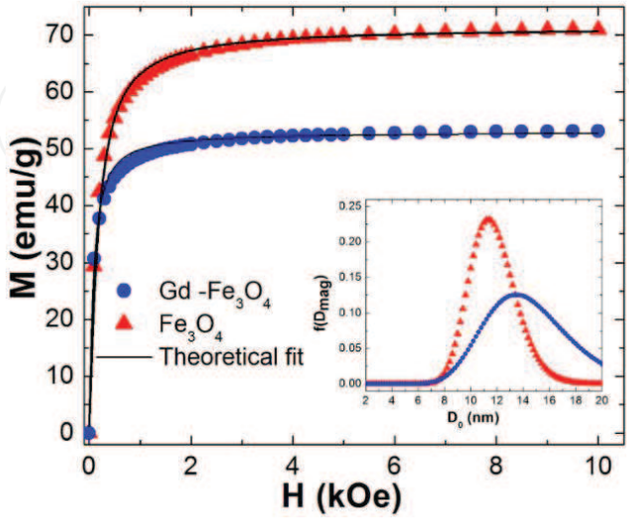

Figure 6. M versus H curves for two ferrofluid samples fitted with Eq. (5). The inset shows the resulting particle size distribution obtained for the two samples [160].

observed XRD data, and it was necessary to introduce the magnetic dipolar interaction effects through a phenomenological temperature, T^*, as described in our recent work [140]. The best-fit parameters for the two samples are shown in **Table 2**, and **Figure 6** shows the fitted data. The inset in **Figure 6** shows the magnetic core size distributions for two ferrofluid samples. The fitting of $M(H)$ data with Eq. (5) clearly shows that Gd-doped Fe_3O_4 nanoparticles have a higher average magnetic core size with a larger size distribution (14.6 ± 3.7 nm) and lower saturation magnetization (52 emu/g) compared to the undoped Fe_3O_4 nanoparticles (11.7 ± 1.9 nm, 72 emu/g). Both the ferrofluid samples exhibit similar strength of magnetic dipolar interaction (T^* ~80–100 K).

MHT measurements were carried out on the dextran-coated Gd-doped as well as undoped Fe_3O_4 ferrofluid samples at a field of 235 Oe and at a frequency of 375 kHz. The heating curves for two samples are shown in **Figure 7(a)**, and from the plot it can be observed that the initial heating rates for the two samples are approximately the same. From these heating curves, the SAR values were obtained as a function of temperature taking into account heat loss as described elsewhere [134]. **Figure 7(b)** presents the corrected experimental SAR data as a function of temperature for both the undoped and Gd-doped samples. Within the experimental error, the room temperature SAR values for Gd-doped Fe_3O_4 and undoped

Ferrofluid sample	M_s (emu/g)	D_o (nm)	σ	T^* (K)	D_{avg} (nm)
Fe_3O_4	72	11.6	0.15	80	11.7 ± 1.9
Gd -Fe_3O_4	52	14.2	0.23	100	14.6 ± 3.7

Table 2. Fitting parameters obtained from the $M(H)$ fitting with modified Langevin function using T^*.

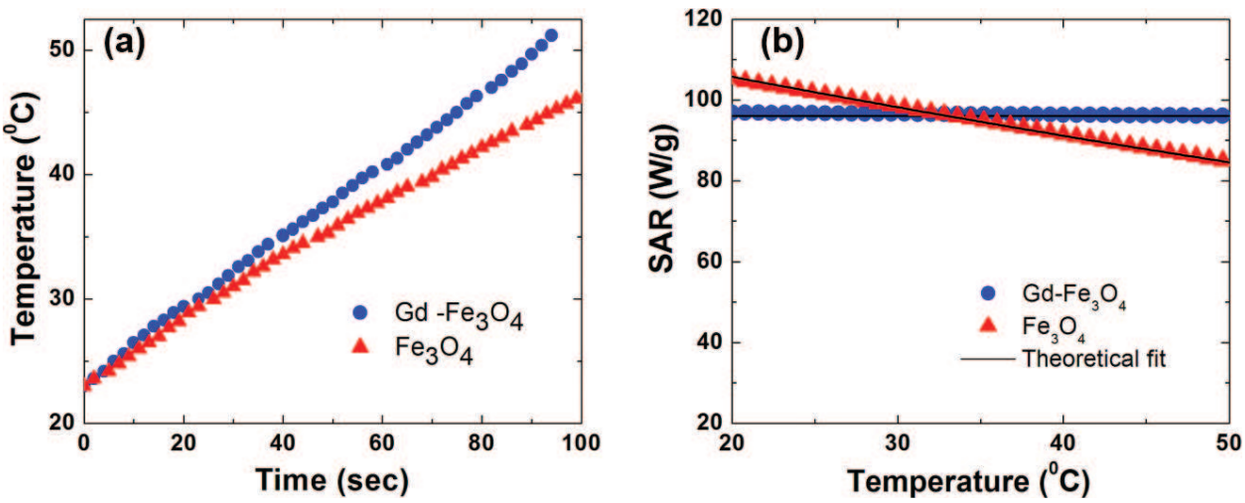

Figure 7. (a) Heating profiles of Fe_3O_4 and Gd-doped Fe_3O_4 ferrofluid samples under an AC magnetic field amplitude of 235 Oe and at a frequency of 375 kHz. (b) The temperature dependence of net SAR for two ferrofluid samples. The black line shows the theoretical fitting of the experimental data with the linear response theory [160].

Fe_3O_4 ferrofluid are very similar. The temperature-dependent SAR values were fitted to the linear response theory incorporated with the interactions and size distribution [140]. The solid lines in **Figure 7(b)** are the best fits to the experimental SAR data, using the particle size distribution parameters and T^* values given in **Table 2** and treating the anisotropy constant, K, as a fitting parameter. The SAR fitting yields a somewhat smaller anisotropy constant (~12 kJ/m^3) for Gd-doped ferrofluid compared to that of undoped ferrofluid (~21kJ/m^3). It is interesting to note that both samples have similar SAR values in spite of a smaller anisotropy constant and the saturation magnetization for the $Gd_{0.075}Fe_{2.925}O_4$ sample compared to the undoped sample. The expected lowering of SAR in $Gd_{0.075}Fe_{2.925}O_4$ is probably offset by a larger particle size in this sample, as the SAR would increase with increasing particle size up to a critical size [140]. By fine-tuning the composition of Gd-doped Fe_3O_4 nanoparticles, we may achieve a higher SAR value.

In summary, the Gd doping on the Fe_3O_4 nanoparticles affects the morphology and the magnetic properties of Fe_3O_4 nanoparticles considerably but the magnetic hyperthermia efficiency of the samples was about the same within the experimental uncertainties. The possibility of using Gd-doped Fe_3O_4 nanoparticles as a dual-modal T_1-T_2 contrast agent is being currently explored by others and our magnetic hyperthermia results demonstrate that this material is a potential candidate for multimodal contrast imaging and cancer treatment by hyperthermia. However, further research is necessary to optimize the amount of Gd doping to enhance SAR for cancer treatment and to be used as a theranostic agent.

8. Conclusions

In this chapter, we have discussed various approaches to exploit the multifunctionality of SPION for cancer theranostics. We have given a brief background on the nanoparticle magnetism, followed by a description of commonly used synthesis methods and surface-functionalizing strategies. Three major applications of Fe_3O_4 nanoparticles in drug delivery, MRI, and MHT, including our recent work on Gd-doped SPION as a possible theranostic agent, are described. This chapter also addresses the recent work on integrating the individual diagnostic and therapeutic approaches to develop SPION-based theranostic platform.

Despite the exciting progress, SPION is far from meeting clinical standards as theranostic agent. It has its own promises and advantages, but there are still some disadvantages to be overcome. These include target specificity as drug carriers, optimizing the heating efficiency and aim for sufficient heating using minimum dosage, preventing the overheating in MHT, and issues of biocirculation, biodistribution, and bioelimination within the biological system. In summary, although in theory, SPION is a perfect vehicle in the development of theranostic nanomedicine, more research is required to overcome its disadvantages and this should be the main focus of the next stages of investigation.

9. Future directions

In recent years, the research in the field of theranostics has brought many diverse fields together for targeting, imaging, and therapy for a deadly disease like cancer. These fields include physics of magnetism, chemistry of synthesis, material science of structure-property relationship, surface science for functionalization, biomedical engineering in MRI and radiofrequency activation and treatment, and biology for understanding the behavior of cancer cells. SPIONs have played a key role in this application as visual, imaging, and therapeutic agent. Several studies have shown promising results; however, many challenges still remain in moving theranostic applications from laboratory settings to clinics. Two major challenges we face are low efficacy and toxicity of SPION. For in vivo applications, the amount of SPION used (several hundred microgram/ml) usually produces undesirable toxic side effects. The smaller concentration, on the other hand, is not sufficient for imagining and therapeutic action of the material. It is well known that the size, shape, and surface modifications influence the performance of SPION. There is a lack of information about the combined effects of these parameters in the clinical applications. Also, we do not have a clear understanding of controlling the delivery of SPION to a specific target in the body by using external magnetic field gradient. It has been found that some particles would end up accumulating in other parts of the body such as liver, spleen, kidney, and lungs along with the specific intended location. We do not know how they will affect those nonspecific organs and how long they will stay there. In magnetic hyperthermia therapy, measuring precise temperature at the tumor site and adjusting particle properties with frequencies and amplitude of the external field for apoptosis/necrosis of cancer cells without affecting normal tissues are challenges that researchers and clinicians face every day. There have been promising results in treating prostate and skin cancers with magnetic fluid hyperthermia but no real efforts have been made to treat deep tumors such a pancreas and liver with SPION. In order to make progress with these therapies, research is needed in the development of new materials that have higher reflexivity, better thermal activation properties, and have better coating materials to improve the bio-distribution and biocompatibility for in vivo applications. Most imperatively, we need data on large animal studies before theranostics can make a fruitful transition from research laboratories to the clinics, and so on.

Acknowledgements

RN would like to thank Richard Barber Foundation for continued research support for this work. PPV would like to thank Kettering University for financial support through multiple Faculty Research Fellowship and Rodes professorship awards.

Author details

Maheshika Palihawadana-Arachchige[1], Vaman M. Naik[2], Prem P. Vaishnava[3], Bhanu P. Jena[4] and Ratna Naik[1]*

*Address all correspondence to: rnaik@wayne.edu

1 Department of Physics and Astronomy, Wayne State University, Detroit, MI, USA

2 Department of Natural Sciences, University of Michigan-Dearborn, Dearborn, MI, USA

3 Kettering University, Flint, MI, USA

4 Department of Physiology, State University, Detroit, MI, USA

References

[1] Portney NG, Ozkan M. Nano-oncology: Drug delivery, imaging, and sensing. Analytical and Bioanalytical Chemistry. 2006;**384**:620–630

[2] Farokhzad OC, Langer R. Nanomedicine: Developing smarter therapeutic and diagnostic modalities. Advanced Drug Delivery Reviews. 2006;**58**:1456–1459

[3] Peer D, Karp JM, Hong S, Farokhzad OC, Margalit R, Langer R. Nanocarriers as an emerging platform for cancer therapy. Nature Nanotechnology. 2007;**2**:751–760

[4] Yoo D, Lee J-H, Shin T-H, Cheon J. Theranostic magnetic nanoparticles. Accounts of Chemical Research. 2011;**44**:863–874

[5] Xie J, Lee S, Chen X. Nanoparticle-based theranostic agents. Advanced Drug Delivery Reviews. 2010;**62**:1064–1079

[6] Veiseh O, Gunn JW, Zhang M. Design and fabrication of magnetic nanoparticles for targeted drug delivery and imaging. Advanced Drug Delivery Reviews. 2010;**62**:284–304

[7] Rosen JE, Chan L, Shieh D-B, Gu FX. Iron oxide nanoparticles for targeted cancer imaging and diagnostics. Nanomedicine Nanotechnology. 2012;**8**:275–290

[8] Xie J, Jon S. Magnetic nanoparticle-based theranostics. Theranostics. 2012;**2**:122–124

[9] Ito A, Shinkai M, Honda H, Kobayashi T. Medical application of functionalized magnetic nanoparticles. Journal of Bioscience and Bioengineering.2005;**100**:1–11

[10] Colombo M, Carregal-Romero S, Casula MF, Gutiérrez L, Morales MP, Böhm IB, Heverhagen JT, Prosperi D, Parak WJ. Biological applications of magnetic nanoparticles. Chemical Society Review. 2012;**41**:4306–4334

[11] Issa B, Obaidat IM, Albiss BA, Haik Y. Magnetic nanoparticles: Surface effects and properties related to biomedicine applications. International Journal of Molecular Science. 2013;**14**:21266–21305

[12] Huang S-H, Juang R-S. Biochemical and biomedical applications of multifunctional magnetic nanoparticles: A review. Journal of Nanoparticle Research. 2011;**13**:4411

[13] Lawes G, Naik R, Vaishnava P. Physical properties and biomedical applications of superparamagnetic iron oxide nanoparticles. Nanocellbiology. 2014:257

[14] Kolhatkar AG, Jamison AC, Litvinov D, Willson RC, Lee TR. Tuning the magnetic properties of nanoparticles. International Journal of Molecular Science. 2013;**14**:15977–16009

[15] Guardia P, Labarta A, Batlle X. Tuning the size, the shape, and the magnetic properties of iron oxide nanoparticles. Journal of Physical Chemistry C. 2011;**115**:390–396

[16] Singamaneni S, Bliznyuk VN, Binek C, Tsymbal EY. Magnetic nanoparticles: Recent advances in synthesis, self-assembly and applications. Journal of Material Chemistry. 2011;**21**:16819–16845

[17] Lu AH, Salabas EEL, Schüth F. Magnetic nanoparticles: Synthesis, protection, functionalization, and application. Angewandte Chemie International Edition. 2007;**46**:1222–1244

[18] Gupta AK, Gupta M. Synthesis and surface engineering of iron oxide nanoparticles for biomedical applications. Biomaterials. 2005;**26**:3995–4021

[19] Pisane KL, Singh S, Seehra MS. Synthesis, structural characterization and magnetic properties of Fe/Pt core-shell nanoparticles. Journal of Applied Physics. 2015;**117**:17d708

[20] Singh V, Seehra MS, Bali S, Eyring EM, Shah N, Huggins FE, Huffman GP. Magnetic properties of (Fe, Fe–B)/γ-Fe_2O_3 core shell nanostructure. Journal of Physics and Chemistry of Solids. 2011;**72**:1373–1376

[21] Seehra MS, Singh V, Dutta P, Neeleshwar S, Chen YY, Chen CL, Chou SW, Chen CC. Size-dependent magnetic parameters of fcc FePt nanoparticles: Applications to magnetic hyperthermia. Journal of Physics D: Applied Physics. 2010;**43**:145002

[22] Pisane KL, Despeaux EC, Seehra MS. Magnetic relaxation and correlating effective magnetic moment with particle size distribution in maghemite nanoparticles. Journal of Magnetism and Magnetic Materials. 2015;**384**:148–154

[23] Seehra MS, Pisane KL. Relationship between blocking temperature and strength of interparticle interaction in magnetic nanoparticle systems. Journal of Physics and Chemistry of Solids. 2016;**93**:79–81

[24] Pankhurst QA, Connolly J, Jones SK, Dobson J. Applications of magnetic nanoparticles in biomedicine. Journal of Physics D: Applied Physics. 2003;**36**:R167

[25] Jun Y-W, Seo J-W, Cheon J. Nanoscaling laws of magnetic nanoparticles and their applicabilities in biomedical sciences. Accounts of Chemical Research. 2008;**41**:179–189

[26] Guardia P, Pérez N, Labarta A, Batlle X. Controlled synthesis of iron oxide nanoparticles over a wide size range. Langmuir. 2010;**26**:5843–5847

[27] Comesaña-Hermo M, Ciuculescu D, Li Z-A, Stienen S, Spasova M, Farle M, Amiens C. Stable single domain Co nanodisks: Synthesis, structure and magnetism. Journal of Material Chemistry. 2012;**22**:8043–8047

[28] Cozzoli PD, Snoeck E, Garcia MA, Giannini C, Guagliardi A, Cervellino A, Gozzo F, Hernando A, Achterhold K, Ciobanu N, Parak FG, Cingolani R, Manna L. Colloidal synthesis and characterization of tetrapod-shaped magnetic nanocrystals. Nano Letters. 2006;**6**:1966–1972

[29] Gao G, Liu X, Shi R, Zhou K, Shi Y, Ma R, Takayama-Muromachi E, Qiu G. Shape-controlled synthesis and magnetic properties of monodisperse Fe_3O_4 nanocubes. Crystal Growth & Design. 2010;**10**:2888–2894

[30] Han GC, Zong BY, Wu YH. Magnetic properties of magnetic nanowire arrays. IEEE Transactions on Magnetics. 2002;**38**:2562–2564

[31] Puntes VF, Zanchet D, Erdonmez CK, Alivisatos AP. Synthesis of hcp-Co nanodisks. Journal of the American Chemical Society. 2002;**124**:12874–12880

[32] Schladt TD, Shukoor MI, Schneider K, Tahir MN, Natalio F, Ament I, Becker J, Jochum FD, Weber S, Köhler O, Theato P, Schreiber LM, Sönnichsen C, Schröder HC, Müller WEG, Tremel W. Au@MnO nanoflowers: Hybrid nanocomposites for selective dual functionalization and imaging. Angewandte Chemie International Edition. 2010;**49**: 3976–3980

[33] Song Q, Zhang ZJ. Shape control and associated magnetic properties of spinel cobalt ferrite nanocrystals. Journal of the American Chemical Society. 2004;**126**:6164–6168

[34] Wu C-G, Lin HL, Shau N-L. Magnetic nanowires via template electrodeposition. Journal of Solid State Electrochemistry. 2006;**10**:198–202

[35] Yan M, Fresnais J, Berret J-F. Growth mechanism of nanostructured superparamagnetic rods obtained by electrostatic co-assembly. Soft Matter. 2010;**6**:1997–2005

[36] Závišová V, Tomašovičová N, Kováč J, Koneracká M, Kopčanský P, Vávra I. Synthesis and characterisation of rod-like magnetic nanoparticles. Olomouc, Czech Republic. 2010;**10**.

[37] Zhao Z, Zhou Z, Bao J, Wang Z, Hu J, Chi X, Ni K, Wang R, Chen X, Chen Z, Gao J. Octapod iron oxide nanoparticles as high-performance T2 contrast agents for magnetic resonance imaging. Nature Communications. 2013;**4**:2266

[38] Salazar-Alvarez G, Qin J, Sepelak V, Bergmann I, Vasilakaki M, Trohidou K, Ardisson J, Macedo W, Mikhaylova M, Muhammed M. Cubic versus spherical magnetic nanoparticles: The role of surface anisotropy. Journal of the American Chemistry Society. 2008;**130**:13234–13239

[39] Noh S-H, Na W, Jang J-T, Lee J-H, Lee EJ, Moon SH, Lim Y, Shin J-S., Cheon J. Nanoscale magnetism control via surface and exchange anisotropy for optimized ferrimagnetic hysteresis. Nano Letters. 2012;**12**:3716–3721

[40] Lee J-H, Huh Y-M, Jun Y-W, Seo J-W, Jang J-T, Song H-T, Kim S, Cho E-J, Yoon H-G, Suh J-S, Cheon J. Artificially engineered magnetic nanoparticles for ultra-sensitive molecular imaging. Nature Medicine. 2007;**13**:95–99

[41] Grasset F, Mornet S, Demourgues A, Portier J, Bonnet J, Vekris A, Duguet E. Synthesis, magnetic properties, surface modification and cytotoxicity evaluation of $Y_3Fe_{5-x}Al_xO_{12}$ ($0 \leqslant x \leqslant 2$) garnet submicron particles for biomedical applications. Journal of Magnetism and Magnetic Materials. 2001;**234**:409–418

[42] Sun S, Zeng H. Size-controlled synthesis of magnetite nanoparticles. Journal of the American Chemistry Society. 2002;**124**:8204–8205

[43] Jana NR, Chen Y, Peng X. Size- and shape-controlled magnetic (Cr, Mn, Fe, Co, Ni) oxide nanocrystals via a simple and general approach. Chemistry of Materials. 2004;**16**:3931–3935

[44] Hyeon T. Chemical synthesis of magnetic nanoparticles. Chemical Communications. 2003:927–934

[45] Roca AG, Costo R, Rebolledo AF, Veintemillas-Verdaguer S, Tartaj P, González-Carreño T, Morales MP, Serna CJ. Progress in the preparation of magnetic nanoparticles for applications in biomedicine. Journal of Physics D: Applied Physics. 2009;**42**:224002

[46] Laurent S, Forge D, Port M, Roch A, Robic C, Vander Elst L, Muller R.N. Magnetic iron oxide nanoparticles: Synthesis, stabilization, vectorization, physicochemical characterizations, and biological applications. Chemical Reviews. 2008;**108**:2064–2110

[47] Mascolo M, Pei Y, Ring T. Room temperature co-precipitation synthesis of magnetite nanoparticles in a large pH window with different bases. Materials. 2013;**6**:5549

[48] Latham AH, Williams ME. Controlling transport and chemical functionality of magnetic nanoparticles. Accounts of Chemical Research. 2008;**41**:411–420

[49] Daou TJ, Pourroy G, Bégin-Colin S, Grenèche JM, Ulhaq-Bouillet C, Legaré P, Bernhardt P, Leuvrey C, Rogez G. Chemistry of materials, hydrothermal synthesis of monodisperse magnetite nanoparticles. American Chemical Society. 2006:4399–4404

[50] Ge S, Shi X, Sun K, Li C, Uher C, Baker JR, Banaszak Holl MM, Orr BG. Facile hydrothermal synthesis of iron oxide nanoparticles with tunable magnetic properties. Journal of Physics and Chemistry C. 2009;**113**:13593–13599

[51] Chin AB, Yaacob II. Synthesis and characterization of magnetic iron oxide nanoparticles via w/o microemulsion and Massart's procedure. Journal of Materials Processing Technology. 2007;**191**:235–237

[52] Wei W, Quanguo H, Hong C, Jianxin T, Libo N. Sonochemical synthesis, structure and magnetic properties of air-stable Fe_3O_4/Au nanoparticles. Nanotechnology. 2007;**18**: 145609

[53] Alexis F, Pridgen E, Molnar LK, Farokhzad OC. Factors affecting the clearance and biodistribution of polymeric nanoparticles. Molecular Pharmaceutics. 2008;**5**:505–515

[54] Knop K, Hoogenboom R, Fischer D, Schubert US. Poly(ethylene glycol) in drug delivery: Pros and cons as well as potential alternatives. Angewandte Chemie International Edition. 2010;**49**:6288–6308

[55] Filippousi M, Angelakeris M, Katsikini M, Paloura E, Efthimiopoulos I, Wang Y, Zamboulis D, Van Tendeloo G. Surfactant effects on the structural and magnetic properties of iron oxide nanoparticles. Journal of Physics and Chemistry C. 2014;**118**:16209–16217

[56] Marín T, Montoya P, Arnache O, Calderón J. Influence of surface treatment on magnetic properties of Fe_3O_4 nanoparticles synthesized by electrochemical method. Journal of Physics and Chemistry B. 2016

[57] Soares PIP, Alves AMR, Pereira LCJ, Coutinho JT, Ferreira IMM, Novo CMM, Borges JPMR. Effects of surfactants on the magnetic properties of iron oxide colloids. Journal of Colloid and Interface Science. 2014;**419**:46–51

[58] Yuan Y, Rende D, Altan CL, Bucak S, Ozisik R, Borca-Tasciuc D-A. Effect of surface modification on magnetization of iron oxide nanoparticle colloids. Langmuir. 2012;**28**: 13051–13059

[59] Salafranca J, Gazquez J, Pérez N, Labarta A, Pantelides ST, Pennycook SJ, Batlle X, Varela M. Surfactant organic molecules restore magnetism in metal-oxide nanoparticle surfaces. Nano Letters. 2012;**122**:499–2503

[60] Duan H, Kuang M, Wang X, Wang YA, Mao H, Nie S. Reexamining the effects of particle size and surface chemistry on the magnetic properties of iron oxide nanocrystals: New insights into spin disorder and proton relaxivity. Journal of Physics and Chemistry C. 2008;**112**:8127–8131

[61] Molday RS, MacKenzie D. Immunospecific ferromagnetic iron-dextran reagents for the labeling and magnetic separation of cells. Journal of Immunological Methods. 1982;**52**: 353–367

[62] Bulte JWM, Ma LD, Magin RL, Kamman RL, Hulstaert CE, Go KG, The TH, De Leij L. Selective MR imaging of labeled human peripheral blood mononuclear cells by liposome mediated incorporation of dextran-magnetite particles. Magnetic Resonance in Medicine. 1993;**29**:32–37

[63] Massia SP, Stark J, Letbetter DS. Surface-immobilized dextran limits cell adhesion and spreading. Biomaterials. 2000;**21**:2253–2261

[64] Weissleder R, Elizondo G, Wittenberg J, Lee AS, Josephson L, Brady TJ. Ultrasmall superparamagnetic iron oxide: An intravenous contrast agent for assessing lymph nodes with MR imaging. Radiology. 1990;**175**:494–498

[65] Josephson L, Tung C-H, Moore A, Weissleder R. High-efficiency intracellular magnetic labeling with novel superparamagnetic-tat peptide conjugates. Bioconjugate Chemistry. 1999;**10**:186–191

[66] Wunderbaldinger P, Josephson L, Weissleder R. Crosslinked iron oxides (CLIO). Academic Radiology. 2002;**9**:S304-S306

[67] Mikhaylova M, Kim DK, Bobrysheva N, Osmolowsky M, Semenov V, Tsakalakos T, Muhammed M. Superparamagnetism of magnetite nanoparticles: Dependence on surface modification. Langmuir. 2044;**20**:2472–2477

[68] Kim DK, Mikhaylova M, Wang FH, Kehr J, Bjelke B, Zhang Y, Tsakalakos T, Muhammed M. Starch-coated superparamagnetic nanoparticles as MR contrast agents. Chemistry of Materials. 2003;**15**:4343–4351

[69] Donadel K, Felisberto MDV, Fávere VT, Rigoni M, Batistela NJ, Laranjeira MCM. Synthesis and characterization of the iron oxide magnetic particles coated with chitosan biopolymer. Material Science Engineering: C. 2008;**28**:509–514

[70] Denkbaş EB, Kiliçay E, Birlikseven C, Öztürk E. Magnetic chitosan microspheres: Preparation and characterization. Reactive and Functional Polymers. 2002;**50**:225–232

[71] Kim EH, Ahn Y, Lee HS. Biomedical applications of superparamagnetic iron oxide nanoparticles encapsulated within chitosan. Journal of Alloys Compounds. 2007;**434-435**:633–636

[72] Khor E, Lim LY. Implantable applications of chitin and chitosan. Biomaterials. 2003;**24**: 2339–2349

[73] Gupta AK, Wells S. Surface-modified superparamagnetic nanoparticles for drug delivery: Preparation, characterization, and cytotoxicity studies. IEEE Transactions on Nano-Bioscience. 2004;**3**:66–73

[74] Zhang Y, Kohler N, Zhang M. Surface modification of superparamagnetic magnetite nanoparticles and their intracellular uptake. Biomaterials. 2002;**23**:1553–1561

[75] Gupta AK, Curtis ASG. Surface modified superparamagnetic nanoparticles for drug delivery: Interaction studies with human fibroblasts in culture. Journal of Materials Science: Materials in Medicine. 2004;**15**:493–496

[76] Sudakar C, Dixit A, Regmi R, Naik R, Lawes G, Naik VM, Vaishnava PP, Toti U, Panyam J. Fe_3O_4 incorporated AOT-alginate nanoparticles for drug delivery. IEEE Transactions on Magnetics. 2008;**44**:2800–2803

[77] Ma HL, Xu YF, Qi XR, Maitani Y, Nagai T. Superparamagnetic iron oxide nanoparticles stabilized by alginate: Pharmacokinetics, tissue distribution, and applications in detecting liver cancers. International Journal of Pharmaceutics. 2008;**354**:217–226

[78] Morales MA, Finotelli PV, Coaquira JAH, Rocha-Leão MHM, Diaz-Aguila C, Baggio-Saitovitch EM, Rossi AM. In situ synthesis and magnetic studies of iron oxide nanoparticles in calcium-alginate matrix for biomedical applications. Materials Science Engineering: C. 2008;**28**:253–257

[79] Wang H, Luo W, Chen J. Fabrication and characterization of thermoresponsive Fe_3O_4@PNIPAM hybrid nanomaterials by surface-initiated RAFT polymerization. Journal of Materials Science. 2012;**47**:5918–5925

[80] Chen G, Hoffman AS. Preparation and properties of thermoreversible, phase-separating enzyme-oligo(N-isopropylacrylamide) conjugates. Bioconjugate Chemistry. 1993;**4**:509–514

[81] Regmi R, Bhattarai SR, Sudakar C, Wani AS, Cunningham R, Vaishnava PP, Naik R, Oupicky D, Lawes G. Hyperthermia controlled rapid drug release from thermosensitive magnetic microgels. Journal of Materials Chemistry. 2010;**20**:6158–6163

[82] Fang J, Wang C, Cao M, Cheng M, Shi J, Jin Y. Preparation and properties of multifunctional Fe_3O_4@PNIPAM-AAM@Au composites. Materials Letters. 2013;**96**:89–92

[83] Park I-K, Ng C-P, Wang J, Chu B, Yuan C, Zhang S, Pun SH. Determination of nanoparticle vehicle unpackaging by MR imaging of a T2 magnetic relaxation switch. Biomaterials. 2008;**29**:724–732

[84] Chorny M, Polyak B, Alferiev IS, Walsh K, Friedman G, Levy RJ. Magnetically driven plasmid DNA delivery with biodegradable polymeric nanoparticles. FASEB Journal. 2007;**21**:2510–2519

[85] Steitz B, Hofmann H, Kamau SW, Hassa PO, Hottiger MO, von Rechenberg B, Hofmann-Amtenbrink M, Petri-Fink A. Characterization of PEI-coated superparamagnetic iron oxide nanoparticles for transfection: Size distribution, colloidal properties and DNA interaction. Journal of Magnetism and Magnetic Materials. 2007;**311**:300–305

[86] McBain SC, Yiu HHP, El Haj A, Dobson J. Polyethyleneimine functionalized iron oxide nanoparticles as agents for DNA delivery and transfection. Journal of Materials Chemistry. 2007;**17**:2561–2565

[87] McBain SC, Yiu HHP, Dobson J. Magnetic nanoparticles for gene and drug delivery. International Journal of Nanomedicine. 2008;**3**:169–180

[88] Wang C, Ravi S, Martinez GV, Chinnasamy V, Raulji P, Howell M, Davis Y, Mallela J, Seehra MS, Mohapatra S. Dual-purpose magnetic micelles for MRI and gene delivery. Journal of Controlled Release. 2012;**163**:82–92

[89] Thevenot J, Oliveira H, Sandre O, Lecommandoux S. Magnetic responsive polymer composite materials. Chemical Society Review. 2013;**42**:7099–7116

[90] Karimi M, Ghasemi A, Sahandi Zangabad P, Rahighi R, Moosavi Basri SM, Mirshekari H, Amiri M, Shafaei Pishabad Z, Aslani A, Bozorgomid M, Ghosh D, Beyzavi A, Vaseghi A, Aref AR, Haghani L, Bahrami S, Hamblin MR. Smart micro/nanoparticles in stimulus-responsive drug/gene delivery systems. Chemical Society Review. 2016;**45**: 1457–1501

[91] Bonini M, Berti D, Baglioni P. Nanostructures for magnetically triggered release of drugs and biomolecules. Current Opinion in Colloid Interface Science. 2013;**18**:459–467

[92] Hayashi K, Ono K, Suzuki H, Sawada M, Moriya M, Sakamoto W, Yogo T. High-frequency, magnetic-field-responsive drug release from magnetic nanoparticle/organic hybrid based on hyperthermic effect. ACS Applied Materials Interfaces. 2010;**2**:1903–1911

[93] Munnier E, Cohen-Jonathan S, Linassier C, Douziech-Eyrolles L, Marchais H, Soucé M, Hervé K, Dubois P, Chourpa I. Novel method of doxorubicin-SPION reversible association for magnetic drug targeting. International Journal of Pharmaceutics. 2008;**363**:170–176

[94] Gautier J, Munnier E, Paillard A, Hervé K, Douziech-Eyrolles L, Soucé M, Dubois P, Chourpa I. A pharmaceutical study of doxorubicin-loaded PEGylated nanoparticles for magnetic drug targeting. International Journal of Pharmaceutics. 2012;**423**:16–25

[95] He X, Wu X, Cai X, Lin S, Xie M, Zhu X, Yan D. Functionalization of magnetic nanoparticles with dendritic-linear-brush-like triblock copolymers and their drug release properties. Langmuir. 2012;**28**:11929–11938

[96] Ying XY, Du YZ, Hong LH, Yuan H, Hu FQ. Magnetic lipid nanoparticles loading doxorubicin for intracellular delivery: Preparation and characteristics. Journal of Magnetism and Magnetic Materials. 2011;**323**:1088–1093

[97] Liao C, Sun Q, Liang B, Shen J, Shuai X. Targeting EGFR-overexpressing tumor cells using Cetuximab-immunomicelles loaded with doxorubicin and superparamagnetic iron oxide. European Journal of Radiology. 2011;**80**:699–705

[98] Quan Q, Xie J, Gao H, Yang M, Zhang F, Liu G, Lin X, Wang A, Eden HS, Lee S, Zhang G, Chen X. HSA coated iron oxide nanoparticles as drug delivery vehicles for cancer therapy. Molecular Pharmaceutics. 2011;**8**:1669–1676

[99] Gu YJ, Cheng J, Man CWY, Wong WT, Cheng SH. Gold-doxorubicin nanoconjugates for overcoming multidrug resistance. Nanomedicine: Nanotechnology. 2012;**8**:204–211

[100] Hua MY, Yang HW, Liu HL, Tsai RY, Pang ST, Chuang KL, Chang YS, Hwang TL, Chang YH, Chuang HC, Chuang CK. Superhigh-magnetization nanocarrier as a doxorubicin delivery platform for magnetic targeting therapy. Biomaterials. 2011;**32**:8999–9010

[101] Berry CC, Curtis AS. Functionalization of magnetic nanoparticles for applications in biomedicine. Journal of Physics D: Applied Physics. 2003;**36**:R198

[102] Chen F-H, Zhang L-M, Chen Q-T, Zhang Y, Zhang Z-J. Synthesis of a novel magnetic drug delivery system composed of doxorubicin-conjugated Fe_3O_4 nanoparticle cores

and a PEG-functionalized porous silica shell. Chemical Communications. 2010;**46**:8633–8635

[103] Nigam S, Chandra S, Newgreen DF, Bahadur D, Chen Q. Poly (ethylene glycol)-modified PAMAM-Fe3O4-doxorubicin triads with the potential for improved therapeutic efficacy: Generation-dependent increased drug loading and retention at neutral pH and increased release at acidic pH. Langmuir. 2014;**30**:1004–1011

[104] Akbarzadeh A, Samiei M, Joo SW, Anzaby M, Hanifehpour Y, Nasrabadi HT, Davaran S. Synthesis, characterization and in vitro studies of doxorubicin-loaded magnetic nanoparticles grafted to smart copolymers on A549 lung cancer cell line. Journal of Nanobiotechnology. 2012;**10**:46

[105] Arachchige MP, Laha SS, Naik AR, Lewis KT, Naik R, Jena BP. Functionalized nanoparticles enable tracking the rapid entry and release of doxorubicin in human pancreatic cancer cells. Micron. 2017;**92**:25–31

[106] Shokrollahi H. Contrast agents for MRI. Material Science Engineering: C. 2013;**33**:4485–4497

[107] Caravan P, Ellison JJ, McMurry TJ, Lauffer RB. Gadolinium (III) chelates as MRI contrast agents: Structure, dynamics, and applications. Chemical Reviews. 1999;**99**:2293–2352

[108] Arsalani N, Fattahi H, Nazarpoor M. Synthesis and characterization of PVP-functionalized superparamagnetic Fe_3O_4 nanoparticles as an MRI contrast agent. Express Polymer Letters. 2010;**4**:329–338

[109] Kim D, Zhang Y, Kehr J, Klason T, Bjelke B, Muhammed M. Characterization and MRI study of surfactant-coated superparamagnetic nanoparticles administered into the rat brain. Journal of Magnetism and Magnetic Materials. 2001;**225**:256–261

[110] Hu F, Wei L, Zhou Z, Ran Y, Li Z, Gao M. Preparation of biocompatible magnetite nanocrystals for in vivo magnetic resonance detection of cancer. Advance Materials. 2006;**18**:2553–2556

[111] Stephen ZR, Kievit FM, Zhang M. Magnetite nanoparticles for medical MR imaging. Material Today. 2011;**14**:330–338

[112] Comparative study of the magnetic behavior of spherical and cubic superparamagnetic iron oxide nanoparticles. Journal of Physics and Chemistry C. 2011;**115**:327–334

[113] Park YC, Smith JB, Pham T, Whitaker RD, Sucato CA, Hamilton JA, Bartolak-Suki E, Wong JY. Effect of PEG molecular weight on stability, T(2) contrast, cytotoxicity, and cellular uptake of superparamagnetic iron oxide nanoparticles (SPIONs). Colloids and Surfaces. B, Biointerfaces. 2014;**119**:106–114

[114] Xie J, Chen K, Lee H-Y, Xu C, Hsu AR, Peng S, Chen X, Sun S. Ultrasmall c(RGDyK)-coated Fe_3O_4 nanoparticles and their specific targeting to integrin $\alpha v\beta 3$-rich tumor cells. Journal of the American Chemical Society. 2008;**130**:7542–7543

[115] Huh Y-M, Jun Y-W, Song H-T, Kim S, Choi J-S, Lee J-H, Yoon S, Kim K-S, Shin J-S, Suh J-S, Cheon J. In vivo magnetic resonance detection of cancer by using multifunctional magnetic nanocrystals. Journal of the American Chemical Society. 2005;**127**:12387–12391

[116] Kim BH, Lee N, Kim H, An K, Park YI, Choi Y, Shin K, Lee Y, Kwon SG, Na HB, Park J-G, Ahn T-Y, Kim Y-W, Moon WK, Choi SH, Hyeon T. Large-scale synthesis of uniform and extremely small-sized iron oxide nanoparticles for high-resolution T1 magnetic resonance imaging contrast agents. Journal of the American Chemical Society. 2011;**133**: 12624–12631

[117] Jun Y-W, Huh Y-M, Choi J-S, Lee J-H, Song H-T, Kim Kim, Yoon S, Kim K-S, Shin J-S, Suh J-S, Cheon J. Nanoscale size effect of magnetic nanocrystals and their utilization for cancer diagnosis via magnetic resonance imaging. Journal of the American Chemical Society. 2005;**127**:5732–5733

[118] De M, Chou SS, Joshi HM, Dravid VP. Hybrid magnetic nanostructures (MNS) for magnetic resonance imaging applications. Advanced Drug Delivery Reviews. 2011;**63**: 1282–1299

[119] Shin T-H, Choi Y, Kim S, Cheon J. Recent advances in magnetic nanoparticle-based multi-modal imaging. Chemical Society Review. 2015;**44**:4501–4516

[120] Bae KH, Kim YB, Lee Y, Hwang J, Park H, Park TG. Bioinspired synthesis and characterization of gadolinium-labeled magnetite nanoparticles for dual contrast T1- and T2-weighted magnetic resonance imaging. Bioconjugate Chemistry. 2010;**21**:505–512

[121] Santra S, Jativa SD, Kaittanis C, Normand G, Grimm J, Perez JM. Gadolinium-encapsulating iron oxide nanoprobe as activatable NMR/MRI contrast agent. ACS Nano. 2012;**6**:7281–7294

[122] Zhou Z, Huang D, Bao J, Chen Q, Liu G, Chen Z, Chen X, Gao J. A synergistically enhanced T1–T2 dual-modal contrast agent. Advanced Materials. 2012;**24**:6223–6228

[123] Xiao N, Gu W, Wang H, Deng Y, Shi X, Ye L. T1–T2 dual-modal MRI of brain gliomas using PEGylated Gd-doped iron oxide nanoparticles. Journal of Colloid and Interface Science. 2014;**417**:159–165

[124] Maenosono S, Saita S. Theoretical assessment of FePt nanoparticles as heating elements for magnetic hyperthermia. IEEE Transactions on Magnetism. 2006;**42**:1638–1642

[125] Gilchrist RK, Medal R, Shorey WD, Hanselman RC, Parrott JC, Taylor CB. Selective inductive heating of lymph nodes. Annals of Surgery. 1957;**146**:596–606

[126] Sonvico F, Mornet S, Vasseur S, Dubernet C, Jaillard D, Degrouard J, Hoebeke J, Duguet E, Colombo P, Couvreur P. Folate-conjugated iron oxide nanoparticles for solid tumor targeting as potential specific magnetic hyperthermia mediators: Synthesis, physicochemical characterization, and in vitro experiments. Bioconjugate Chemistry. 2005;**16**: 1181–1188

[127] Sharifi I, Shokrollahi H, Amiri S. Ferrite-based magnetic nanofluids used in hyperthermia applications. Journal of Magnetism and Magnetic Materials. 2012;**324**:903–915

[128] Pereira C, Pereira AM, Fernandes C, Rocha M, Mendes R, Fernández-García MP, Guedes A, Tavares PB, Grenèche J-M, Araújo JOP. Superparamagnetic MFe_2O_4 (M= Fe, Co, Mn) nanoparticles: Tuning the particle size and magnetic properties through a novel one-step coprecipitation route. Chemistry of Materials. 2012;**24**:1496–1504

[129] Lasheras X, Insausti M, Gil de Muro I, Garaio E, Plazaola F, Moros M, De Matteis L, de la Fuente JSM, Lezama L. Chemical synthesis and magnetic properties of monodisperse nickel ferrite nanoparticles for biomedical applications. Journal of Physics and Chemistry C. 2016;**120**:3492–3500

[130] Dutz S, Kettering M, Hilger I, Müller R, Zeisberger M. Magnetic multicore nanoparticles for hyperthermia—Influence of particle immobilization in tumour tissue on magnetic properties. Nanotechnology. 2011;**22**:265102

[131] Vasseur S, Duguet E, Portier J, Goglio G, Mornet S, Hadová E, Knížek K, Maryško M, Veverka P, Pollert E. Lanthanum manganese perovskite nanoparticles as possible in vivo mediators for magnetic hyperthermia. Journal of Magnetism and Magnetic Materials. 2006;**302**:315–320

[132] Jang JT, Nah H, Lee JH, Moon SH, Kim MG, Cheon J. Critical enhancements of MRI contrast and hyperthermic effects by dopant-controlled magnetic nanoparticles. Angewandte Chemie. 2009;**121**:1260–1264

[133] Miller KJ, Sofman M, McNerny K, McHenry ME. Metastable γ-FeNi nanostructures with tunable Curie temperature. Journal of Applied Physics. 2010;**107**:09A305

[134] Nemala H, Thakur JS, Naik VM, Vaishnava PP, Lawes G, Naik R. Investigation of magnetic properties of Fe_3O_4 nanoparticles using temperature dependent magnetic hyperthermia in ferrofluids. Journal of Applied Physics. 2014;**116**:034309

[135] Rosensweig RE. Heating magnetic fluid with alternating magnetic field. Journal of Magnetism and Magnetic Materials. 2002;**252**:370–374

[136] Effect of nanoclustering and dipolar interactions in heat generation for magnetic hyperthermia. Langmuir. 2016;**32**:1201–1213

[137] Branquinho LC, Carrião MS, Costa AS, Zufelato N, Sousa MH, Miotto R, Ivkov R, Bakuzis AF. Effect of magnetic dipolar interactions on nanoparticle heating efficiency: Implications for cancer hyperthermia. Scientific Reports. 2013;**3**:2887

[138] Landi GT. Role of dipolar interaction in magnetic hyperthermia. Physics Review B. 2014;**89**:014403

[139] Sadat ME, Patel R, Sookoor J, Bud'ko SL, Ewing RC, Zhang J, Xu H, Wang Y, Pauletti GM, Mast DB, Shi D. Effect of spatial confinement on magnetic hyperthermia via dipolar interactions in Fe_3O_4 nanoparticles for biomedical applications. Materials Science Engineering: C. 2014;**42**:52–63

[140] Palihawadana-Arachchige M, Nemala H, Naik VM, Naik R. Effect of magnetic dipolar interactions on temperature dependent magnetic hyperthermia in ferrofluids. Journal of Applied Physics. 2017;**121**:023901

[141] Mohammad F, Balaji G, Weber A, Uppu RM, Kumar CS. Influence of gold nanoshell on hyperthermia of superparamagnetic iron oxide nanoparticles. Journal of Physics and Chemistry C. 2010;**114**:19194–19201

[142] Liu XL, Fan HM, Yi JB, Yang Y, Choo ESG, Xue JM, Fan DD, Ding J. Optimization of surface coating on Fe_3O_4 nanoparticles for high performance magnetic hyperthermia agents. Journal of Material Chemistry. 2012;**22**:8235–8244

[143] Cedervall T, Lynch I, Lindman S, Berggård T, Thulin E, Nilsson H, Dawson KA, Linse S. Understanding the nanoparticle–protein corona using methods to quantify exchange rates and affinities of proteins for nanoparticles. Proceedings of the National Academy of Sciences of the United States of America. 2007;**104**:2050–2055

[144] Klein J. Probing the interactions of proteins and nanoparticles. Proceedings of the National Academy of Sciences of the United States of America. 2007;**104**:2029–2030

[145] Khan S, Gupta A, Nandi CK. Controlling the fate of protein corona by tuning surface properties of nanoparticles. Journal of Physics and Chemistry Letters. 2013;**4**:3747–3752

[146] Calatayud MP, Sanz B, Raffa V, Riggio C, Ibarra MR, Goya GF. The effect of surface charge of functionalized Fe_3O_4 nanoparticles on protein adsorption and cell uptake. Biomaterials. 2014;**35**:6389–6399

[147] Khandhar AP, Ferguson RM, Krishnan KM. Monodispersed magnetite nanoparticles optimized for magnetic fluid hyperthermia: Implications in biological systems. Journal of Applied Physics. 2011;**109**:07B310

[148] Drug-loaded superparamagnetic iron oxide nanoparticles for combined cancer imaging and therapy in vivo. Angewendte Chemie International Edition. 2008;**47**:5362–5365

[149] Uniform mesoporous dye-doped silica nanoparticles decorated with multiple magnetite nanocrystals for simultaneous enhanced magnetic resonance imaging, fluorescence imaging, and drug delivery. Journal of the American Chemical Society. 2010;**132**:552–557.

[150] Kim J, Kim HS, Lee N, Kim T, Kim H, Yu T, Song IC, Moon WK, Hyeon T. Multifunctional uniform nanoparticles composed of a magnetite nanocrystal core and a mesoporous silica shell for magnetic resonance and fluorescence imaging and for drug delivery. Angewendte Chemie. 2008;**120**:8566–8569

[151] Thomas R, Park I-K, Jeong Y. Magnetic iron oxide nanoparticles for multimodal imaging and therapy of cancer. International Journal of Molecular Science. 2013;**14**:15910

[152] Hayashi K, Nakamura M, Sakamoto W, Yogo T, Miki H, Ozaki S, Abe M, Matsumoto T, Ishimura K. Superparamagnetic nanoparticle clusters for cancer theranostics combining magnetic resonance imaging and hyperthermia treatment. Theranostics. 2013;**3**:366–376

[153] Hilger I, Kaiser WA. Iron oxide-based nanostructures for MRI and magnetic hyperthermia. Nanomedicine. 2012;**7**:1443–1459

[154] Bozorth RM, Williams HJ, Walsh DE. Magnetic properties of some orthoferrites and cyanides at low temperatures. Physics Reviews. 1956;**103**:572–578

[155] Litsardakis G, Manolakis I, Efthimiadis K. Structural and magnetic properties of barium hexaferrites with Gd–Co substitution. Journal of Alloys and Compound. 2007;**427**:194–198

[156] Panda RN, Shih JC, Chin TS. Magnetic properties of nano-crystalline Gd- or Pr-substituted $CoFe_2O_4$ synthesized by the citrate precursor technique. Journal of Magnetism and Magnetic Materials. 2003;**257**:79–86

[157] Jiang P-S, Drake P, Cho H-J, Kao C-H, Lee K-F, Kuo C-H, Lin X-Z, Lin Y-J. Tailored nanoparticles for tumour therapy. Journal of Nanoscience and Nanotechnology. 2012;**12**:5076–5081

[158] Drake P, Cho H-J, Shih P-S, Kao C-H, Lee K-F, Kuo C-H, Lin X-Z, Lin Y-J. Gd-doped iron-oxide nanoparticles for tumour therapy via magnetic field hyperthermia. Journal of Materials Chemistry. 2007;**17**:4914–4918

[159] Peng J, Hojamberdiev M, Xu Y, Cao B, Wang J, Wu H. Hydrothermal synthesis and magnetic properties of gadolinium-doped $CoFe_2O_4$ nanoparticles. Journal of Magnetism and Magnetic Materials. 2011;**323**:133–137

[160] Palihawadana-Arachchige M, Naik V, Naik R. Gd doped Fe_3O_4 nanoparticles for magnetic hyperthermia and MRI. To be published.

IntechOpen